Paediatric interventional cardiology: flat detector versus image intensifier using a test object

2010 Phys. Med. Biol. 55 7287

(http://iopscience.iop.org/0031-9155/55/23/007)

IOP PUBLISHING PHYSICS IN MEDICINE AND BIOLOGY

Phys. Med. Biol. **55** (2010) 7287–7297 doi:10.1088/0031-9155/55/23/007

Paediatric interventional cardiology: flat detector versus image intensifier using a test object

E Vano[1], C Ubeda[2], L C Martinez[3], F Leyton[4] and P Miranda[5]

[1]Radiology Department, Medicine School, Complutense University and San Carlos University Hospital, 28040 Madrid, Spain
[2]Clinical Sciences Department, Faculty of the Science of Health and CIHDE, Tarapaca University, 18 de Septiembre 2222, Arica, Chile
[3]Medical Physics and Radiation Protection Service, 12 de Octubre University Hospital, Madrid, Spain
[4]Institute of Public Health of Chile, Marathon 1000, Nunoa, Santiago, Chile
[5]Hemodynamic Department, Cardiovascular Service, Luis Calvo Mackenna Hospital, Avenida Antonio Varaas 360, Providencia, Santiago, Chile

E-mail: eliseov@med.ucm.es

Received 19 July 2010, in final form 7 September 2010
Published 16 November 2010
Online at stacks.iop.org/PMB/55/7287

Abstract

Entrance surface air kerma (ESAK) values and image quality parameters were measured and compared for two biplane angiography x-ray systems dedicated to paediatric interventional cardiology, one equipped with image intensifiers (II) and the other one with dynamic flat detectors (FDs). Polymethyl methacrylate phantoms of different thicknesses, ranging from 8 to 16 cm, and a Leeds TOR 18-FG test object were used. The parameters of the image quality evaluated were noise, signal-difference-to-noise ratio (SdNR), high contrast spatial resolution (HCSR) and three figures of merit combining entrance doses and signal-to-noise ratios or HCSR. The comparisons showed a better behaviour of the II-based system in the low contrast region over the whole interval of thicknesses. The FD-based system showed a better performance in HCSR. The FD system evaluated would need around two times more dose than the II system evaluated to reach a given value of SdNR; moreover, a better spatial resolution was measured (and perceived in conventional monitors) for the system equipped with flat detectors. According to the results of this paper, the use of dynamic FD systems does not lead to an automatic reduction in ESAK or to an automatic improvement in image quality by comparison with II systems. Any improvement also depends on the setting of the x-ray systems and it should still be possible to refine these settings for some of the dynamic FDs used in paediatric cardiology.

1. Introduction

Patient doses are influenced by many factors at the catheterization laboratories and several studies show that entrance surface air kerma (ESAK) values during interventional cardiology (IC) procedures are influenced by the type and setting of angiography x-ray systems and the different acquisition modes used (Bor *et al* 2006, Vano *et al* 2005).

Radiation doses in paediatrics require special attention because of the higher radiosensitivity of the patients (Bacher *et al* 2005). The risk of cancer induction by ionizing radiation is two to three times higher for infants and children than for adults (ICRP 2007).

Several papers reporting phantom (or patient) doses and image quality for IC in adults have been published and some of them deal with x-ray systems equipped with image intensifiers (II) and dynamic flat panel detectors (FDs) (Holmes *et al* 2004, Tsapaki *et al* 2004, Bor *et al* 2006, Davies *et al* 2007, Mesbahi *et al* 2008). Nevertheless, the publications for IC in paediatrics are scarce.

In modern angiography systems equipped with II, a charge-coupled device (CCD) replaces the old tube camera and allows more imaging capabilities. Dynamic FDs, based on large arrays of amorphous silicon photodiodes and thin film transistors in combination with CsI(Tl) scintillators, have the potential to improve image quality with less radiation dose than II (Vano *et al* 2005, Davies *et al* 2007).

Technical comparison between FDs and II has shown advantages of better ergonomics with better patient access, insensitivity to magnetic fields, wider dynamic range, the availability of distortion-free images and an excellent contrast resolution (Grewal and McLean 2005, Spahn 2005). Some of these advantages can directly be associated with patient dose savings (Bokou *et al* 2008).

The goal of this study is to compare ESAK values and some image quality parameters evaluated from a test object (TO), for two biplane angiography x-ray systems dedicated to paediatric IC, one equipped with IIs and the other one with dynamic FDs. The comparison was made using polymethyl methacrylate (PMMA) phantoms of different thicknesses to simulate paediatric patients.

2. Material and methods

The measurements were made in two biplane angiography x-ray systems used for IC in paediatrics: Siemens Axiom Artis BC equipped with II and Siemens Axiom Artis dBC equipped with two dynamic FDs[6].

For the one equipped with II, with a generator of 100 kW at 100 kV, three fluoroscopy modes were available: low (FL), medium (FM) and high dose (FH). All of them were configured in pulsed mode at 15 pulses s^{-1}. Cine mode (CI) was typically used at 30 frames s^{-1}. The system had three fields of view (FOV): 16, 22 and 33 cm. Additional filters, from 0.1 to 0.9 mmCu and virtual collimation were available. The isocentre to the floor distance was 107 cm and the focus to the isocentre distance was 76 cm. The system included internal selectable post-processing software called dynamic density optimization (DDO).

The FD system was equipped with amorphous silicon detectors of 25 cm in diagonal dimension and pixel size of 184 μm. It also had a generator of 100 kW at 100 kV. Three fluoroscopy modes were available: FL, FM and FH, all of them configured at 15 pulses s^{-1}, whereas cine mode was used at 30 frames s^{-1}. The selectable FOVs were 16, 20 and 25 cm (diagonal dimension). Additional filters from 0.1 to 0.9 mmCu, virtual collimation and DDO

[6] http://www.medical.siemens.com

were also available in this system. The isocentre to the floor distance was 106 cm and the focus to the isocentre distance was 75 cm.

2.1. ESAK evaluations

The DIMOND and SENTINEL European protocols were used to characterize both x-ray systems (Faulkner *et al* 2008, Simon *et al* 2008), but in our case they were adapted to paediatric procedures. PMMA plates of dimensions 25 cm × 25 cm × 1 cm (2 and 3 cm) were employed to build thicknesses of 8, 12 and 16 cm to simulate paediatric patients. FOVs of 22 and 25 cm were used for II and FD, respectively, considering that they are the most common FOVs used in paediatrics. The comparison of image quality was made with the cine acquisition modes using a specific protocol setting the DDO parameter to zero. The II system was used only for paediatric cardiology, and the different acquisition protocols were configured by the Siemens engineer: newborn, infant and child. The FD system, however, was also used for other procedures, in addition to paediatric cardiology, and had only one acquisition mode available called 'paediatric'.

A solid-state detector Unfors Xi (model 8201010-A) with a measurement probe (model 82020030-AXi)[7] in contact with the PMMA plates was used to measure incident air kerma (IAK) (ICRU 2005) for the II system. It was placed inside the radiation beam but not in the automatic exposure control (AEC) area. To facilitate the comparison of our results to other measurements, a backscatter (BS) factor 1.3 was used to calculate the ESAK (ICRU 2005). As for the system with dynamic FDs, a flat ionization chamber (model 20 × 6–60) with a 2026C radiation meter from RadCal[8] in contact with the PMMA plates was used to measure ESAK (with BS). Both dosimetry systems (solid-state detector and flat ionization chamber) were duly calibrated, traceable to official calibration laboratories[9,10]. Entrance image detector doses were measured without removing the antiscatter grid and in contact with the grid.

For a PMMA thickness of 4 cm and with the TO at the isocentre, the floor-to-tabletop distance was 104 cm. The table-to-solid-state detector (or ionization chamber for the FD system) distance was 1 cm. The tabletop-to-isocentre distance was 3 cm and the focus-to-detector distance was 74 cm. For 8, 12 and 16 cm of PMMA, this distance was decreased to 72, 70 and 68, respectively, to maintain the TO at the isocentre (the table was moved down 2 cm when 4 cm of PMMA was added). The II (or FD) was always kept 5 cm from the top side of the PMMA slab (also to simulate typical clinical working conditions).

Typically, in the cardiac systems (with image intensifiers), the 'active' region for AEC is set to 40–50% of the central area of the detector. For FDs, this criterion changes depending on different software releases. In our case, we have tested during the experiment that when the detector was in the periphery of the radiation field the main radiographic parameters (kV, mA and filtration) demonstrated no appreciable changes.

2.2. Image quality evaluation

A TO (Leeds TOR 18-FG)[11] was positioned at the isocentre, in the middle of the PMMA thickness, during all the measurements, thus providing the best geometry to simulate real clinical conditions. The image acquisition format was in both x-ray systems

[7] http://www.unfors.com/products.php?catid = 19
[8] http://www.radcal.com
[9] Unfors instruments AB. Certificate no: 142527–20071031. Sweden.
[10] The John Perry Radiation Metrology Laboratory, St George's Hospital, London, UK.
[11] http://www.leedstestobjects.com/products/tor/product-tor-18 fg.htm, Leeds, UK.

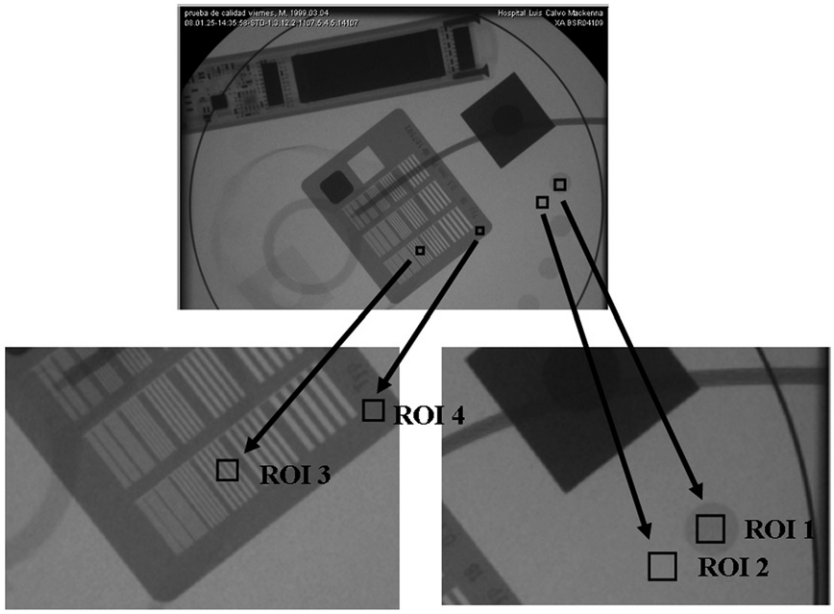

Figure 1. Example of how the numerical evaluation was performed. Image corresponds to 'cine' acquisition mode with the II system, FOV 22 cm, PMMA thickness 20 cm. ROI 1 used for the 'signal' and ROI 2 for the background; ROIs 3–4 used to evaluate the HCSR parameter. The rectangular structure that appears in the upper side of the image is the solid-state detector.

1024 × 1024 pixels and 12 bits before compression. The image recording format, after compression, was the standard for cardiology: 512 × 512 pixels and 8 bits. The image detector (II or FD) was placed 5 cm away from the PMMA surface.

The image quality was evaluated with four numerical parameters (see the definitions below): noise (N) (Huda *et al* 2003), signal-difference-to-noise ratio (SdNR) (Samei *et al* 2005), figure of merit (FOM) (Samei *et al* 2005) and high-contrast spatial resolution (HCSR) (Vano *et al* 2008). The SdNR had previously been used by some authors as SNR (signal-to-noise ratio) (Van Engen *et al* 2006) or CNR (contrast-to-noise ratio) (Huda *et al* 2003). This numerical evaluation was always performed on three images (numbers 5, 8 and 10 of the cine series avoiding the first images to guarantee a proper adjustment of the AEC), to calculate in each case the mean values and the maximum deviations (MDs) between the three images, evaluated. Osiris software, version 4.18[12], was used to evaluate the images with an IBM corporation Intel® Pentium® M processor 1.73 GHz, 198 MHz, 760 MB of RAM (with a screen mode of 1024 × 768 pixels, IBM ThinkPad LCD Mobile Intel® 915GMGMS).[13]

The numerical parameters selected to evaluate the image quality were defined as (see figure 1 for further details) follows.

1. Noise, N (Huda *et al* 2003):

$$N = \frac{\mathrm{SD_{BG}}}{\mathrm{BG}}, \tag{1}$$

where $\mathrm{SD_{BG}}$ is the corresponding standard deviation for the pixel content in a rectangular region of interest near the low contrast circle number 1 (ROI 2), see figure 1. BG is the

[12] http://www.sim.hcuge.ch/osiris/01 Osiris Presentation EN.htm
[13] http://www.ibm.com/es/

background value, the mean value of the pixel content in a rectangular region of interest near the low contrast circle number 1 (ROI 2) and of the same size as the ROI selected from inside the circle (figure 1).

2. Signal-difference-to-noise ratio, SdNR (Samei *et al* 2005):

$$\mathrm{SdNR} = \frac{|\mathrm{BG} - \mathrm{ROI}|}{\mathrm{SD_{BG}}}, \tag{2}$$

where ROI is the mean value of the pixel content in a rectangular region of interest inside the circle number 1 (ROI 1), see figure 1.

3. High contrast spatial resolution, HCSR:

$$\mathrm{HCSR} = \mathrm{SD}_1 - \mathrm{SD}_2, \tag{3}$$

where SD_1 is the standard deviation for the pixel content in the ROI 3 (figure 1), inside the seventh group (arbitrary election to facilitate the numerical evaluation) in the central grid of TO. SD_2 is the standard deviation for the pixel content in the ROI 4 (figure 1), selected in the periphery of the high contrast groups and representative of the noise in this area.

4. Figures of merit, FOM (Samei *et al* 2005):

$$\mathrm{FOM_{ESAK}} = \frac{\mathrm{SdNR}^2}{\mathrm{ESAK}} \tag{4}$$

$$\mathrm{FOM_{DD}} = \frac{\mathrm{SdNR}^2}{\mathrm{DD}} \tag{5}$$

$$\mathrm{FOM} = \frac{\mathrm{HCSR}^2}{\mathrm{ESAK}}, \tag{6}$$

where ESAK is measured at the point where the x-ray beam axis enters the PMMA. DD is the detector (entrance air) dose. Nominal values for DD, according to the specifications (included in the DICOM header) have been used.

3. Results

Table 1 shows the most relevant radiographic parameters adjusted by the AEC of both x-ray systems (II and FD) and the measured values of ESAK for the different PMMA thicknesses.

Table 2 shows the image quality parameters measured for both x-ray systems (II and FD) and the different PMMA thicknesses.

In table 1, most of the values are taken from the DICOM header of the x-ray systems as transferred once the fluoroscopy runs or the cine series have been acquired. The two last columns in table 1 are the experimental values. An inaccuracy of 10% could be attributed to these values. Typically, for ESAK measurements, without changing the geometry, the inaccuracy is <3%, but considering that in the II system the measured quantity has been IAK instead of ESAK, we estimate the total inaccuracy for ESAK values within 10% when using the BS factor.

The U Mann–Whitney test has been applied to the full set of our experimental results (ESAK and image quality parameters for the FD and II systems). Values of $p < 0.05$ were considered statistically significant. For ESAK no statistical significant global difference between the FD and II systems existed (with the particular setting of the evaluated units) ($p = 0.954$). For image quality parameters, there are significant differences ($p < 0.004$) for the three parameters: noise, SdNR and HCSR.

Table 1. Tube potential (kVp), tube current (mA), added filter (mmCu), detector dose (nGy/pulse, from DICOM header) and ESAK for all exam protocol, all acquisition modes and all PMMA thicknesses used in both x-ray systems (FD and II). FL = fluoroscopy low; FM = fluoroscopy medium; FH = fluoroscopy high; CI = cine acquisition.

PMMA (cm)	Exam protocol for FD	Exam protocol for II	Acquisition mode	Tube potential for FD (kVp)	Tube potential for II (kVp)	Tube current for FD (mA)	Tube current for II (mA)	Filter for FD (mmCu)	Filter for II (mmCu)	Detector for dose FD (nGy/fr)	Detector for dose II (nGy/fr)	ESAK for FD (μGy/fr)	ESAK for II (μGy/fr)
8	Paediatric	Infant	FL	69.0	77.0	15.0	15.0	0.9	0.9	15.0	15.0	0.36	0.32
8	Paediatric	Infant	FM	76.0	77.0	15.0	22.0	0.9	0.9	33.0	32.0	0.62	0.65
8	Paediatric	Infant	FH	58.0	58.0	128.0	143.0	0.9	0.9	46.0	45.0	1.65	1.52
8	Paediatric	Infant	CI	63.0	63.0	291.0	367.0	0.6	0.6	174.0	170.0	5.77	5.14
12	Paediatric	Child	FL	77.0	77.0	15.0	24.0	0.9	0.9	16.0	15.0	1.11	0.80
12	Paediatric	Child	FM	77.0	77.0	26.0	36.0	0.9	0.9	33.0	32.0	2.39	1.67
12	Paediatric	Child	FH	*	66.0	*	75.0	*	0.6	*	45.0	4.78	3.63
12	Paediatric	Child	CI	67.0	67.0	238.0	334.0	0.3	0.3	162.0	169.0	24.9	17.7
16	Paediatric	Child	FL	77.0	77.0	27.0	39.0	0.9	0.9	15.0	15.0	1.59	2.09
16	Paediatric	Child	FM	77.0	77.0	46.0	61.0	0.9	0.9	34.0	32.0	3.41	4.27
16	Paediatric	Child	FH	66.0	66.0	104.0	146.0	0.6	0.6	43.0	45.0	7.50	10.0
16	Paediatric	Child	CI	68.0	70.0	364.0	399.0	0.2	0.1	165.0	170.0	44.8	63.7

*Not available.

Table 2. Noise, SdNR, standard deviation for the seventh group in HCSR and figure of merit using ESAK (FOM_{ESAK}, FOM) and DD (FOM_{DD}) for cine acquisition mode and exam protocol and all PMMA thicknesses used in the study for both x-ray systems (FD and II).

PMMA (cm)	X-ray system	Noise x 100	SdNR	HCSR	FOM_{ESAK} ($nGy^{-1}(fr)$)	FOM_{DD} ($nGy^{-1}(fr)$)	FOM ($nGy^{-1}(fr)$)
8	FD	1.27 ± 0.08	8.4 ± 0.3	7.3 ± 0.3	12.2 ± 0.9	0.40 ± 0.03	9.2 ± 0.3
	II	0.92 ± 0.10	11.3 ± 1.4	6.1 ± 0.0	25.1 ± 6.3	0.76 ± 0.19	7.6 ± 1.0
12	FD	1.41 ± 0.05	7.1 ± 0.4	6.4 ± 0.2	2.0 ± 0.2	0.31 ± 0.03	1.6 ± 0.2
	II	0.95 ± 0.12	10.7 ± 1.4	6.0 ± 0.1	6.5 ± 1.6	0.68 ± 0.17	2.0 ± 0.0
16	FD	1.21 ± 0.11	7.7 ± 0.4	5.7 ± 0.6	1.3 ± 0.1	0.36 ± 0.04	0.73 ± 0.03
	II	0.88 ± 0.07	11.1 ± 0.8	4.7 ± 0.4	2.0 ± 0.2	0.73 ± 0.10	0.33 ± 0.04

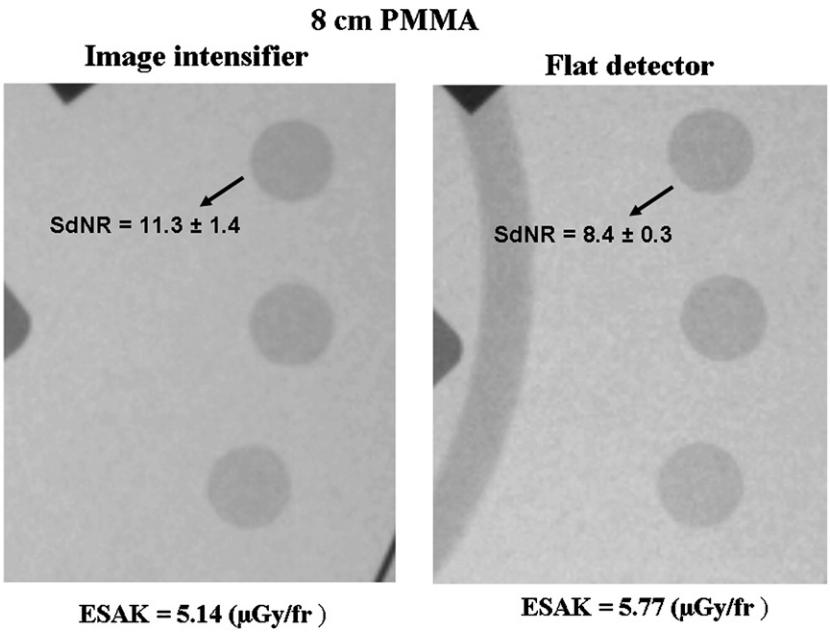

Figure 2. SdNR and ESAK values for II (left) and FD (right) in cine acquisition and a thickness of 8 cm PMMA. The structure that appears in the right image is the wall of the ionization chamber.

Figures 2–4 show examples of low contrast circles and high contrast bar groups obtained for both x-ray systems for 8 cm and 16 cm PMMA.

4. Discussion

According to the results shown in table 1, entrance doses per frame in fluoroscopy and cine acquisition are different in both systems. The II system (for the evaluated configuration) seems to deliver lower dose values for the thicknesses of 8 cm PMMA and 12 cm PMMA, with an average decrease of about 17% compared to the FD system (also, for the particular evaluated configuration), whereas the FD system registers smaller doses for the thickness of 16 cm PMMA, with an average decrease of about 25%. It could roughly be said that the

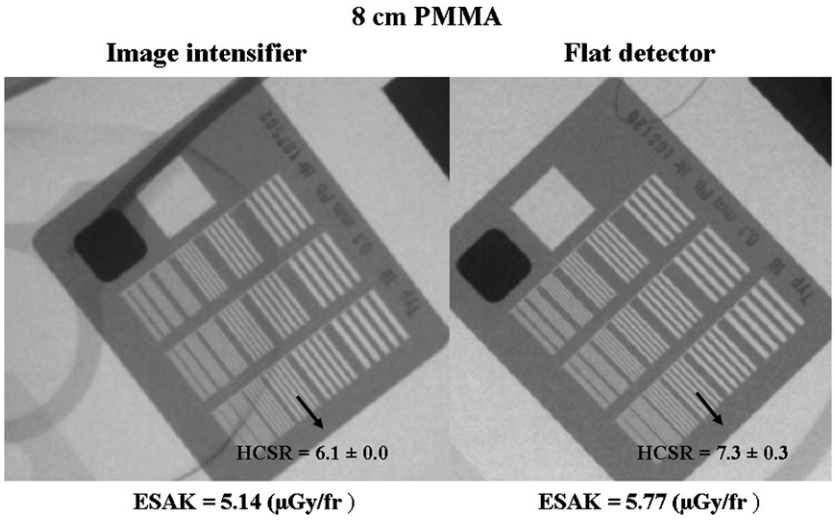

Figure 3. HCSR and ESAK values for II (left) and FD (right) in cine acquisition and a thickness of 8 cm PMMA.

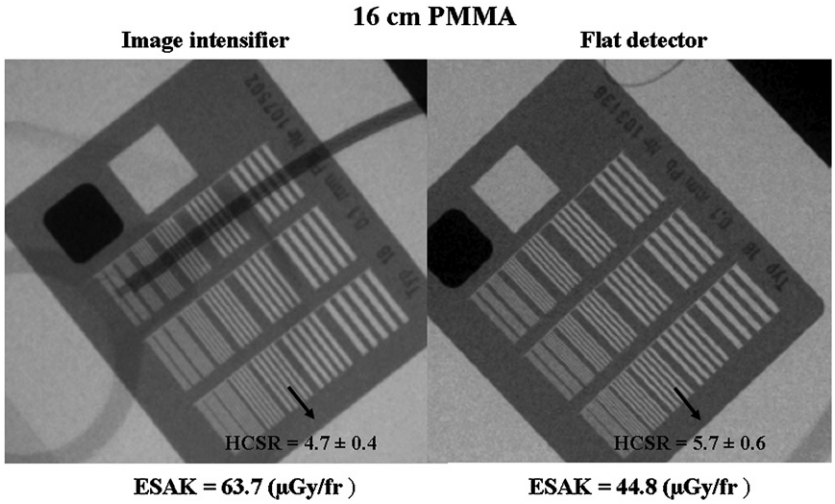

Figure 4. HCSR and ESAK values for II (left) and FD (right) in cine acquisition and a thickness of 16 cm PMMA.

II system seems to be better adjusted for paediatrics as far as the dose is concerned. This could be related to the fact that three different protocols for paediatrics (newborn, infant and child) were available in the II system, whereas only one mode was available in the FD system. Notwithstanding, when comparing the ESAK values for all the operation modes and all the PMMA thicknesses the global difference between the two systems is not statistically significant. Nevertheless, the impact of these small differences on doses to patients in clinical practice is likely to be negligible. Several authors (Tsapaki *et al* 2004, Trianni and Padovani 2005, Davies *et al* 2007) have shown that differences in entrance dose rates bigger than those

found in this paper do not imply a reduction of patient doses during clinical procedures, which confirms the importance of both the operation modes and the skills of the cardiologists. Anyhow, in the case of a same operator using the system with the same acquisition protocol, it seems obvious that, if the x-ray system is set with lower dose/frame and the image quality is good enough, the patient doses should be decreased.

Between 8 cm PMMA and 16 cm, SdNR values for the II system vary by less than 3%, while for the FD system this variation is less than 8%. Both values are reasonable if we take into account that the ESAK per frame increases by a factor of 12 (from 5.14 to 63.7 μGy/frame) for the II system and of 8 (from 5.77 to 44.8 μGy/frame) for the FD system (see tables 1 and 2). However, SdNR values are bigger for the II system than for the FD system over the whole range of thicknesses. Noise values are also lower for the II system than for the FD system (around a 40%). This difference in image quality for the low contrast region can be clearly observed in figure 2, in spite of the loss of image quality of the printed pictures compared to the original ones.

When applying the statistical *U* Mann–Whitney test for all the operation modes and the three thicknessess of PMMA used for the experiment, the differences for noise, SdNR and HCSR are significant.

Table 2 shows better values of $\mathrm{FOM_{DD}}$ and $\mathrm{FOM_{ESAK}}$ for the II system over the whole interval of thicknesses. Note that the conditions kVp/filter established by the AEC for both systems are the same for 8 and 12 cm PMMA and very similar for 16 cm PMMA. This implies that the values of the corresponding FOMs refer to the same beam quality. As a result, it seems that for the systems evaluated and with the existing settings, the FD system would need around two times more dose than the II system to reach a given value of SdNR for a given spectrum (the average ratio of the FOMs).

It has to be noted that, when thicknesses increase, the differences in the values of the FOMs decrease between both systems. This would mean that the II system analysed gives better results than the FD system for paediatrics when dose as well as SNR in the low contrast region are taken into account. But these results should by no means be extrapolated to adult protocols.

Moreover, a better behaviour in the high contrast region has resulted for the FD system, as can be appreciated in figures 3 and 4. Values of the HCSR parameter are bigger in this case in the whole range. When we consider the FOM for this parameter, it shows better values for the FD system over the whole interval of thicknesses (except for 12 cm of PMMA).

Several authors had already reported that the adoption of FD technology would not automatically lead to dose benefits or image quality improvement. Trianni and Padovani (2005) reported an inferior low-contrast resolution and a higher spatial resolution for the FD system as compared to the II system. The evaluation of the image quality was carried out using a Leeds 18-FG test object in a subjective way, with different observers judging the perceptibility of low contrast discs and high contrast line pairs in the phantom. The two systems compared in that case were made by different manufacturers (II by Philips and FD by General Electric), which make the results even more difficult to interpret. Tsapaki *et al* (2004) compared two models of the system Philips Integris Allura and found higher doses in the FD version, compared to the CCD-based version, and similar image qualities. Davies *et al* (2007) indicated that, despite higher performance for FD over II, neither a better image quality nor a reduction of dose to patients was observed under clinical conditions. All these results are consistent with the ones given in this paper.

However, other authors have reported different findings. Bogaert *et al* (2009) found a better image quality in cinegraphy mode for a FD version of a Siemens Axiom Artis monoplane system as compared to the II version of the same system, although not for the fluoroscopy

range. In this case, a phantom of 20 cm PMMA was used to simulate an adult patient. Vano *et al* (2005) also reported an improvement of image quality in cine acquisition set for adult protocols in cardiology in a Siemens Axiom Artis initially installed with II and later upgraded with a dynamic FD. These two studies are especially interesting because while they both refer to Siemens Axiom Artis systems, they differ from our findings. Our entrance dose rates for cine acquisition (paediatric range) are comparable to the fluoroscopy rates measured by Bogaert (adult protocol), due to the smaller thicknesses of our phantoms. Notwithstanding, our doses correspond to the cinegraphy range (80–400 nGy/pulse), which makes our results different from the Bogaert's and Vano's previous findings.

5. Conclusions

The use of dynamic FD systems does not lead to an automatic reduction in ESAK or to an automatic improvement in image quality and does not mean an improvement when compared to II systems. This improvement depends on the setting of the x-ray systems and the results of the present paper demonstrate that refinements should be made in the settings of the dynamic FD used in paediatric cardiology.

Acknowledgments

The authors thank the Mr Bernard Geiger (Siemens AG, Healthcare Sector, D-91301 Forchheim, Germany) for his fruitful discussions and comments on this paper. EV acknowledges the support of the Spanish grant SAF2009-10485 (Ministry of Science and Innovation). CU acknowledges the support of the Direction of Research at Tarapaca University through senior research project no 7713-10.

References

Bacher K, Bogaert E, Lapere R, De Wolf D and Thierens H 2005 Patient-specific dose and radiation risk estimation in pediatric cardiac catheterization *Circulation* **111** 83–9

Bogaert E, Bacher K, Lapere R and Thierens H 2009 Does digital flat detector technology tip the scale towards better image quality or reduced patient dose in interventional cardiology? *Eur. J. Radiol.* **72** 348–53

Bokou C, Schreiner-Karoussou, Breisch R and Beissel J 2008 Changing from image intensifier to flat detector technology for interventional cardiology procedures: a practical point of view *Radiat. Prot. Dosim.* **129** 83–6

Bor D, Toklu T, Olgar T, Sancak T, Cekirge S, Onal B and Bilgic S 2006 Variations of patient doses in interventional examinations at different angiographic units *Cardiovasc. Intervent. Radiol.* **29** 797–806

Davies A, Cowen A, Kengyelics S, Moore J and Sivananthan M 2007 Do flat detector cardiac x-ray systems convey advantages over image-intensifier based systems? Study comparing x-ray dose and image quality *Eur. Radiol.* **17** 1787–94

Faulkner K, Malone J, Vano E, Padovani R, Busch H P, Zoetelief J H and Bosmans H 2008 The SENTINEL Project *Radiat. Prot. Dosim.* **129** 3–5

Grewal R and McLean I 2005 Comparative evaluation of an II based and a flat panel based cardiovascular fluoroscopy system within a clinical environment *Australas. Phys. Eng. Sci. Med.* **28** 151–8

Holmes DR, Laskey WK, Wondrow MA and Cusma JT 2004 Flat-panel detectors in the cardiac catheterization laboratory: revolution or evolution-what are the issues? *Catheter. Cardiovasc. Interv.* **63** 324–30

Huda W, Sajewicz A and Ogden K 2003 Experimental investigation of the dose and image quality characteristics of a digital mammography imaging system *Med. Phys.* **30** 442–8

ICRU 2005 Patient dosimetry for x rays used in medical imaging *ICRU Report 74* (Bethesda, MD: International Commission on Radiological Units and Measurements)

ICRP 2007 The Recommendations of the International Commission on Radiological Protection *ICRP Publication 103 Ann. ICRP* **37** 1–332

Mesbahi A, Mehnati P, Keshtkar A and Aslanabadi N 2008 Comparison of radiation dose to patient and staff for two interventional cardiology units: a phantom study *Radiat. Prot. Dosim.* **131** 399–403

Samei E, Dobbins J, Lo J and Tornai M 2005 A framework for optimising the radiographic technique in digital x-ray imaging *Radiat. Prot. Dosim.* **114** 220–9

Simon R, Vano E, Prieto C, Fernandez JM, Ordiales JM and Martinez D 2008 Criteria to optimise a dynamic flat detector system used for interventional radiology *Radiat. Prot. Dosim.* **129** 261–4

Spahn M 2005 Flat detectors and their clinical applications *Eur. Radiol.* **15** 1934–47

Trianni G and Padovani R 2005 Are new technologies always reducing patient doses in cardiac procedures? *Radiat. Prot. Dosim.* **117** 97–101

Tsapaki V, Kottou S, Kollaros N, Dafnomili P, Koutelou M, Vano E and Neofotistou V 2004 Comparison of a conventional and a flat-panel digital system in interventional cardiology procedures *Br. J. Radiol.* **77** 562–7

Van Engen R, Young K, Bosmans H and Thijsen M 2006 The European protocol for the quality control of physical and technical aspects of mammography screening *Part B Digital Mammography, 4th edn, European Guidelines for Breast Cancer Screening. Luxembourg, European Communities*

Vano E, Geiger B, Schreiner A, Back C and Beissel J 2005 Dynamic flat panel detector versus image intensifier in cardiac imaging: dose and image quality *Phys. Med. Biol.* **7** 5731–42

Vano E, Ubeda C, Leyton F and Miranda P 2008 Radiation dose and image quality for paediatric interventional cardiology *Phys. Med. Biol.* **53** 4049–62